

SCIENTIFIC REPORTS



OPEN

A high throughput approach for the generation of orthogonally interacting protein pairs

Justin Lawrie¹, Xi Song¹, Wei Niu² & Jiantao Guo¹

In contrast to the nearly error-free self-assembly of protein architectures in nature, artificial assembly of protein complexes with pre-defined structure and function *in vitro* is still challenging. To mimic nature's strategy to construct pre-defined three-dimensional protein architectures, highly specific protein-protein interacting pairs are needed. Here we report an effort to create an orthogonally interacting protein pair from its parental pair using a bacteria-based *in vivo* directed evolution strategy. This high throughput approach features a combination of a negative and a positive selection. The newly developed negative selection from this work was used to remove any protein mutants that retain effective interaction with their parents. The positive selection was used to identify mutant pairs that can engage in effective mutual interaction. By using the cohesin-dockerin protein pair that is responsible for the self-assembly of cellulosome as a model system, we demonstrated that a protein pair that is orthogonal to its parent pair could be readily generated using our strategy. This approach could open new avenues to a wide range of protein-based assembly, such as biocatalysis or nanomaterials, with pre-determined architecture and potentially novel functions and properties.

Although significant progress has been made in recent years^{1–14}, the precise manipulation of artificial self-assembly of protein complexes *in vitro* remains a great challenge. In contrast, highly ordered permanent or transient protein complexes widely exist in nature and participate in virtually every type of cellular function, including catalysis, structural support, bodily movement, signal transduction, transport, etc. Nature's error-free self-assembly of protein architectures, such as virus capsids¹⁵, bacterial carboxysomes¹⁶, and cellulosomes (Fig. 1)^{17–19} is driven by many weak, noncovalent interactions at protein-protein interfaces²⁰. The geometry of subunits in a protein complex is precisely defined by those specific noncovalent interactions¹³. In order to mimic nature's strategy to construct highly defined three-dimensional protein architectures, we need to have highly specific protein-protein interacting pairs, analogous to G-C and A-T base-pairing interactions in DNA. One potential solution is to explore naturally occurring protein pairs, such as the barnase and barstar pair²¹. The other potential approach is to artificially generate mutually orthogonal protein pairs from a known parent protein pair. This could further expand the repertoire of highly specific protein pairs that are available for the assembly of protein complexes. In addition, such evolved protein pairs are orthogonal but consist of high sequence homology to the parent protein pair and, therefore, have similar physical/chemical properties. This may minimize certain complications when protein pairs with very different properties are used in the assembly of a protein complex.

To demonstrate the feasibility of the aforementioned approach, we selected a type-I cohesin-dockerin pair from *Clostridium thermocellum* as our model system. High affinity cohesin-dockerin interactions are the basis of self-assembly of cellulosomes^{17,18}, which are multi-protein complexes from certain anaerobic bacteria and fungi for a highly efficient degradation of cellulosic material (Fig. 1). A cellulosome consists of a core structural protein (scaffoldin) that serves as a scaffold to connect multiple catalytic enzymes through the interaction between the type I cohesin domains on itself and the type I dockerin domains of catalytic enzymes. Due to the indiscriminatory nature of cohesin-dockerin recognition within a microorganism species, the assembled cellulosomes have diverse molecular composition and structure, which corresponds to heterogeneous catalytic activities for cellulosic material degradation. In this work, we seek to generate a mutant cohesin-dockerin pair (Fig. 2A) that is derived from but orthogonal to the naturally occurring (wild-type) one. The generation of orthogonal

¹Department of Chemistry, University of Nebraska-Lincoln, Lincoln, Nebraska, 68588, United States. ²Department of Chemical & Biomolecular Engineering, University of Nebraska-Lincoln, Lincoln, Nebraska, 68588, United States. Justin Lawrie and Xi Song contributed equally to this work. Correspondence and requests for materials should be addressed to W.N. (email: wniu2@unl.edu) or J.G. (email: jguo4@unl.edu)

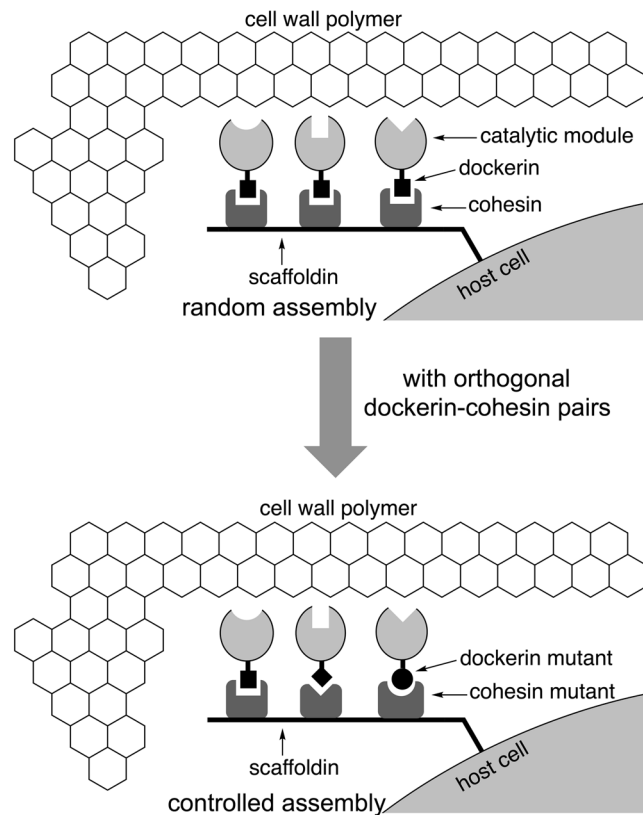


Figure 1. Random and controlled assembly of cellulosome. In nature, the assembly of cellulosomes is mediated by a random attachment of a catalytic module (enzyme), through its dockerin domain, to any cohesin positions on the scaffold protein (scaffoldin). The generation of mutant cohesin-dockerin pairs that are orthogonal to the naturally occurring one may allow a controlled assembly of cellulosomes.

cohesin-dockerin pairs will allow controlled assembly of cellulosomes (Fig. 1), which will facilitate current studies of synergistic actions among cellulosomal enzymes^{17–19}. The second cohesin domain from the scaffoldin protein (CipA; residues 182–328) and the dockerin domain from a glycoside hydrolase (xylanase 10B; residues 733–791) were used in this study. The crystal structure of the protein complex of these two domains has been reported²².

A few methods have been developed for a high-throughput engineering of protein-protein interactions. Phage²³, yeast²⁴, and bacterial²⁵ displayed protein libraries are generally screened with either panning or fluorescence-activated cell sorting (FACS). In contrast, the yeast two-hybrid system²⁶ links protein-protein interactions to a phenotype (e.g., cell growth) that confers a selective advantage to the host, which simplifies the selection process. Bacterial two-hybrid system^{27–29} has also been developed. In comparison to the yeast system, the bacterial system has the advantage of higher transformation efficiency and faster cell growth rate. However, the current bacterial system lacks a negative (counter) selection scheme. In the present study, we devised a bacterial negative selection scheme (Fig. 3B) that is analogous to the yeast one^{30,31}. We subsequently demonstrated that an orthogonal mutant pair could be readily obtained through a combination of positive and negative selections (Fig. 3). Throughout the article, we will use Coh_{wt}-Doc_{wt} and Coh₁-Doc₁ to represent the parent (wild-type) and mutant (evolved) cohesin-dockerin pairs, respectively.

Results and Discussion

General approach. In order to generate a mutant cohesin-dockerin pair that is orthogonal to its parent pair, we explored a structure-guided, semi-rational protein engineering approach (Fig. 2). This approach consists of two essential steps: (1) mutagenesis. The important amino acid residues at the protein-protein interface of the parent pair are randomized. Presumably, such modification would completely abolish or significantly weaken the interaction between mutants and their parents; and (2) selection. This process identifies mutant protein pairs that interact to each other, but do not have significant cross interaction with the parent protein pair. Our selection system consists of both a positive selection and a negative selection (Fig. 3). The positive selection selects mutant cohesin-dockerin pairs that can engage in effective interaction (Fig. 3A). The negative selection removes any dockerin or cohesin mutants that retain effective interaction with the parent cohesin or dockerin (Fig. 3B). The combination of negative and positive selection should yield interacting protein pairs that are orthogonal to their parent (Fig. 3C). This selection scheme can likely be generalized and used to create orthogonal pairs for other proteins as well.

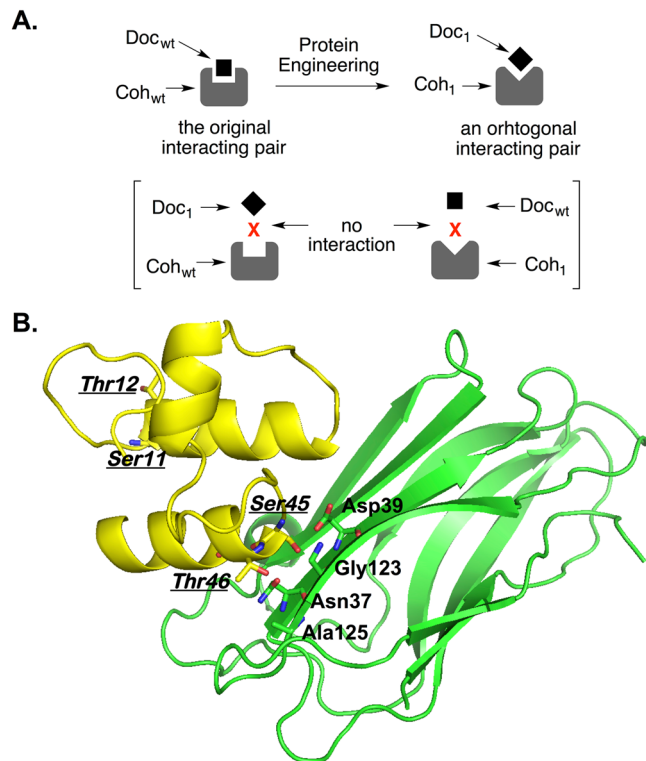


Figure 2. Generation of orthogonal protein pairs from a parent protein pair. **(A)** Generation of mutant dockerin-cohesin ($\text{Doc}_1\text{-Coh}_1$) pair that is orthogonal to the parental $\text{Doc}_{\text{wt}}\text{-Coh}_{\text{wt}}$ pair; **(B)** Structures of $\text{Doc}_{\text{wt}}\text{-Coh}_{\text{wt}}$ pair from *C. thermocellum*. Residues from dockerin (yellow) are labeled in italic and underlined. Residues from cohesin (green) are labeled in regular bold.

Positive selection system. The BacterioMatch[®] II two-hybrid system^{27–29} was used as the molecular biology platform for the positive selection (Fig. 3A). Two reasons promoted us to choose bacteria (*E. coli*) two-hybrid over yeast two-hybrid as the positive selection system: (1) *E. coli* grows much faster than yeast; (2) *E. coli* is transformed with higher efficiency so larger libraries can be readily constructed and selected/screened. BacterioMatch II selection is built upon the genetic complementation of the chromosomal *hisB* gene deletion by the episomal expression of the *S. cerevisiae HIS3* gene in an *E. coli* host strain. Both genes encode imidazoleglycerol-phosphate dehydratase, which is an essential enzyme in the L-histidine biosynthesis. To study the interaction between a cohesin and a dockerin protein, the cohesin is expressed as a C-terminal fusion protein to the full-length bacteriophage λ repressor protein (λCI), and the dockerin is fused to the N-terminal domain of the α -subunit of RNA polymerase ($\text{RNAP}\alpha$). When both fusion proteins are co-expressed in *E. coli* selection host, if the cohesin and the dockerin variants interact, they recruit and stabilize the binding of RNA polymerase at the promoter and activate the transcription of the *HIS3* reporter gene, which allows cells to grow in the presence of 3-amino-1,2,4-triazole (3-AT), a competitive inhibitor of *HIS3* gene product. In general, a stronger interaction confers the cells resistant to higher concentrations of 3-AT, while lack of interaction only permits cells to survive on media without 3-AT. It should be noted that other factors, such as the protein expression level, may affect the cell growth as well. For example, a protein pair with higher expression level can likely survive higher concentrations of 3-AT than a protein pair with lower expression level. If one would like to compare the interaction strength between two different protein pairs by using the positive selection system, the expression levels of the two pairs need to be adjusted to a similar level (e.g., to manipulate gene transcription level using different concentrations of inducer such as IPTG).

To test if the positive selection works, we examined the interaction between the $\text{Coh}_{\text{wt}}\text{-Doc}_{\text{wt}}$ pair. To this end, two plasmids were constructed, including pBT- Coh_{wt} (containing the gene that encodes the $\lambda\text{CI-Coh}_{\text{wt}}$ fusion protein) and pTRG- Doc_{wt} (containing the gene that encodes the $\text{RNAP}\alpha\text{-Doc}_{\text{wt}}$ fusion protein). We initially examined a construct in which Doc_{wt} was directly fused to $\text{RNAP}\alpha$. However, we observed poor cell growth in a two-hybrid study of the $\text{Coh}_{\text{wt}}\text{-Doc}_{\text{wt}}$ interaction. We hypothesized that such poor cell growth was resulted from the degradation of the $\text{RNAP}\alpha\text{-Doc}_{\text{wt}}$ fusion protein since it was known that dockerin domain is prone to degradation in *Escherichia coli*²². According to literature, dockerin-containing enzymes could be expressed as full-length proteins in *E. coli*^{32–35}, we decided to improve the stability of the dockerin protein by inserting the X6b carbohydrate-binding domain between $\text{RNAP}\alpha$ and the dockerin domain. The X6b domain is naturally fused to the N-terminus of the type I dockerin domain from *C. thermocellum* and does not interact with the cohesin domain^{18,19}. The X6b domain was included in all dockerin constructs in this work. As shown in Table 1, cell growth was observed in the presence of 5 mM of 3-AT when both pBT- Coh_{wt} and pTRG- Doc_{wt} were co-transformed into the *E. coli* selection host (entry 1; Table 1). As negative controls, no cell growth was detected when either pBT- Coh_{wt} was co-transformed with the empty pTRG vector or the pTRG- Doc_{wt} was co-transformed

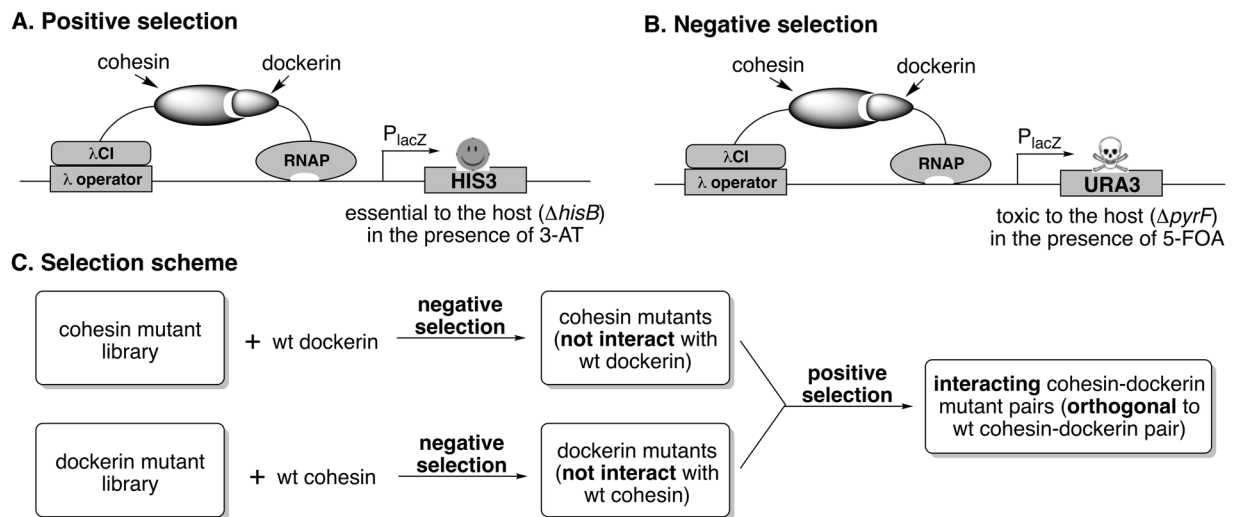


Figure 3. Selection scheme. (A) positive selection; (B) negative selection; (C) selection scheme. The positive selection selects mutant cohesin-dockerin pairs that can engage in effective interaction. The negative selection removes any dockerin or cohesin mutants that retain effective interaction with the parent cohesin or dockerin. The combination of negative and positive selection should yield interacting protein pairs that are orthogonal to their parent. Abbreviations: λ CI, bacteriophage λ repressor protein; RNAP, α -subunit of RNA polymerase; P_{lacZ} , the lac operon promoter; 3-AT, 3-amino-1,2,4-triazole; 5-FOA, 5-fluoroorotic acid.

entry	plasmids in the selection host	cell growth (cfu ^a)	
		0 mM 3-AT	5 mM 3-AT
1	pBT-Coh _{wt} and pTRG-Doc _{wt}	$\sim 5 \times 10^3$	$\sim 1 \times 10^3$
2	pBT and pTRG-Doc _{wt}	$\sim 6 \times 10^3$	0
3	pBT-Coh _{wt} and pTRG	$\sim 5 \times 10^3$	0
4	pTRG-Gal11P and pBT-LGF2	$\sim 6 \times 10^3$	$\sim 1 \times 10^3$
5	pBT-Coh _{wt} and pTRG-Doc _{AL}	$\sim 5 \times 10^3$	0

Table 1. Examination of Coh_{wt} and Doc_{wt} interaction using The BacterioMatch® II two-hybrid system as the positive selection. ^acfu, colony-forming unit.

with the empty pBT vector (entry 2, 3; Table 1). The results confirmed that cells only grew when both Coh_{wt} and Doc_{wt} proteins were present. In comparison to the positive control provided by the BacterioMatch® II kit, the interaction between Coh_{wt} and Doc_{wt} (entry 1; Table 1) led to similar level of cell growth as the interaction between Gal11P and LGF2 (entry 4; Table 1), which were co-expressed from the pTRG-Gal11P and the pBT-LGF2 positive control plasmids.

Negative selection system. As a critical component to enable the generation of orthogonally interacting protein pairs, we developed a negative selection method (Fig. 2B). We modified the yeast URA3/5-FOA counter selection system^{30,31} into the bacterial two-hybrid system. URA3 encodes orotidine 5'-phosphate decarboxylase, which catalyzes the transformation of 5-fluoroorotic acid (5-FOA) into a highly toxic compound (5-fluorouracil) and causes cell death. A similar approach was demonstrated in a bacterial one-hybrid system to select for Zn finger proteins³⁶.

To enable the selection, we first deleted the *pyrF* gene (encodes orotidine-5'-phosphate decarboxylase) on the chromosome of the BacterioMatch II reporter strain to generate strain WNPPI7. As a result, *E. coli* WNPPI7 lost the ability to convert 5-fluoroorotic acid (5-FOA) into a cytotoxic compound, and therefore survives on solid minimal media containing 5-FOA and uracil supplementation (Entry 3, 4; Table 2). We then modified the F' plasmid of WNPPI7 to replace the *HIS3* reporter gene with a copy of the *URA3* gene, resulting in strain WNPPI5. However, the 5-FOA tolerance test showed that the basal expression level of URA3 protein in strain WNPPI5 is high enough to lead to cell death of the host strain itself on plates containing 0.5 mM of 5-FOA (Entry 5, 6; Table 2). To solve the problem, we constructed strain WNPPI8, in which the *URA3* gene was inserted behind the *HIS3* reporter gene. As the second gene in an operon, the reduced basal expression level of URA3 in strain WNPPI8 allowed the cells to survive on plates containing 2.5 mM of 5-FOA (Entry 7; Table 2). When an interacting protein pair (LGF2 and Gal11P) was expressed in strain WNPPI8, the increased transcription level of URA3 resulted in cell death in the presence of as low as 0.5 mM of 5-FOA (Entry 8; Table 2). The negative selection system was further evaluated when pBT-Coh_{wt} and pTRG-Doc_{wt} were co-transformed into WNPPI8. 5-FOA

	host	protein pair	cell growth (cfu ^a) with or without 5-FOA (mM)		
			0	0.5	2.5
1	BacterioMatch II	none	$\sim 1 \times 10^3$	0	0
2	BacterioMatch II	Gal11P and LGF2	$\sim 1 \times 10^3$	0	0
3	WNPP17	none	$\sim 1 \times 10^3$	$\sim 1 \times 10^3$	$\sim 1 \times 10^3$
4	WNPP17	Gal11P and LGF2	$\sim 1 \times 10^3$	$\sim 1 \times 10^3$	$\sim 1 \times 10^3$
5	WNPP15	none	$\sim 1 \times 10^3$	$\sim 10^2$ (tiny ^b)	0
6	WNPP15	Gal11P and LGF2	$\sim 1 \times 10^3$	0	0
7	WNPP18	none	$\sim 1 \times 10^3$	$\sim 1 \times 10^3$	$\sim 1 \times 10^3$
8	WNPP18	Gal11P and LGF2	$\sim 1 \times 10^3$	0	0
9	WNPP18	Coh _{wt} and Doc _{wt}	$\sim 1 \times 10^3$	0	0
10	WNPP18	Coh _{wt} and Doc _{AL}	$\sim 1 \times 10^3$	$\sim 1 \times 10^3$	$\sim 1 \times 10^3$

Table 2. Examination of negative selection host strains^a. ^acfu, colony-forming unit. ^bIn comparison to the regular colony size (~ 1 mm) from other tests, these colonies (< 0.1 mm) were barely seen by eye.

concentrations ranging from 0 mM to 2.5 mM were included in the experiment. In comparison to cell growth on plates without 5-FOA, a significant decrease in colony formation unit was observed when the cells were cultured on plates containing 0.2 mM 5-FOA (data not shown). Further increasing the 5-FOA concentration to either 0.5 or 2.5 mM completely eliminated cell growth (Entry 9, Table 2). As controls, no growth defect was observed when WNPP18 was transformed with either pBT-Coh_{wt} plus pTRG or pTRG-Doc_{wt} plus pBT. The results showed that the URA3/5-FOA negative selection system could efficiently eliminate interacting cohesin and dockerin variants that are generated in the mutagenesis step.

Construction of dockerin and cohesin libraries. Structural data (PDB code, 1OHZ; Fig. 1B)²² revealed that the recognition mechanism of the cohesin-dockerin pair from *C. thermocellum* is mainly mediated by polar interactions^{22,37}. The two highly conserved serine-threonine motifs (Ser11/Thr12 and Ser45/Thr46) in dockerin serve as key recognition codes for binding to the cohesin domain^{38,39}. Due to a near perfect internal two-fold symmetry of dockerin structure (Fig. 2B), the two serine-threonine motifs interact with cohesin domains in a similar manner and only one motif interacts with cohesin at one time. Both literature data⁴⁰ and our experimental observations showed that dockerin mutants with mutations in only one of the two motifs still recognize wild-type cohesin with no apparent decrease in affinity. However, it was reported that mutations in both motifs caused a significant reduction in affinity of the dockerin mutant toward the wild-type cohesin⁴⁰. To further verify this notion, we generated a dockerin mutant (named as Doc_{AL}), which contained four mutations, Ser11Ala, Thr12Leu, Ser45Ala, and Thr46Leu, in the serine-threonine motifs. We showed that Doc_{AL} did not have strong interaction with Coh_{wt} (entry 5; Table 1 and entry 10 Table 2).

In order to obtain dockerin mutants that abolish interaction with wild-type cohesin but can potentially recognize a cohesin mutant, we generated a dockerin mutant library in which four residues (Ser11, Thr12, Ser45, and Thr46) in the two Ser/Thr motifs were fully randomized. We also generated a cohesin mutant library in which four residues (Asn37, Asp39, Gly123, and Ala125) that could potentially affect the recognition of the Ser/Thr motif of dockerin were randomized. NNK codons (N = A, C, T, or G, K = T or G; 32 variants at nucleotide level) were used to cover all 20 amino acids at each mutation site. While mutations into certain amino acid residue(s) may affect the stability and/or expression level of the resulting mutants, such effect is in general hard to predict, and therefore is not taken into consideration in the library construction process. Since most of the amino acid residues are encoded by more than one codon, this design leverages concerns of codon bias-caused difference in protein expression and experimental challenges of constructing large mutant libraries. Both the dockerin and the cohesin library had a diversity of 1.05×10^6 at the nucleotide level. The dockerin mutant library was cloned into the pTRG vector to generate pTRG-Doc_{lib} in which dockerin mutants were fused to the RNAP α protein. The cohesin mutant library was cloned into the pBT vector to generate pBT-Coh_{lib} in which cohesin mutants were fused to the λ CI protein.

Identification of an orthogonal cohesin-dockerin pair through library selections. The dockerin library was first subjected to one round of negative selection against Coh_{wt} in order to eliminate dockerin mutants that retained effective interaction with Coh_{wt}. Surviving cells should contain dockerin mutants that were either non-functional or lost the ability to recognize Coh_{wt}. Similarly, the cohesin library was subjected to one round of negative selection against Doc_{wt} in order to eliminate cohesin mutants that retained effective interaction with Doc_{wt}. Surviving cells should contain cohesin mutants that were either non-functional or lost the ability to recognize Doc_{wt}. It should also be noted that some mutants that can engage in effective interaction with Coh_{wt} or Doc_{wt} might survive the negative selection if their expression levels were too low to induce a sufficient level of URA3 expression. While such possibility exists, these mutants will likely be eliminated in the positive selection due to their low expression levels.

By using plates containing 2.5 mM FOA, the survival rate of the dockerin and cohesin mutants was estimated to be 10–20%. This number was based on the comparison between the control plate (no FOA) and the selection plate (with 2.5 mM FOA; Figure S3). We subsequently examined if we could identify cohesin mutants from the reduced cohesin library after negative selection to engage functional interaction with the aforementioned

	Doc _{wt} -Coh _{wt}	Doc ₁ -Coh ₁	Doc _{wt} -Coh ₁	Doc ₁ -Coh _{wt}
K _d (nM)	0.77 ± 0.10	4.57 ± 1.61	>500	>500

Table 3. K_d values of cohesin-dockerin pairs.

Doc_{AL} mutant. To our delight, a large number of colonies were obtained after one round of positive selection between Doc_{AL} and the reduced cohesin library. We arbitrarily picked eight colonies with different sizes for DNA sequencing analysis. Seven distinct sequences were obtained, while cohesin mutants 3 and 7 converged to the same sequence (Table S2). To estimate the effectiveness of the negative selection and to eliminate false positives (e.g., beneficial host mutations) identified in the positive selection, the pBT-Coh plasmids of the seven distinctive mutants were isolated and reintroduced into the positive selection hosts that harbored either pTRG-Doc_{wt} or pTRG-Doc_{AL}. We observed that all seven mutants engaged in strong interactions with Doc_{AL} and supported cell growth in the presence of 7.5 mM 3-AT. On the other hand, six out of the seven mutants were not able to support cell growth when Doc_{wt} was co-expressed. Apparently, these cohesin mutants did not interact with Doc_{wt}, which indicated that our established negative selection protocol was highly effective.

We arbitrarily picked cohesin mutant 1 (Coh₁; Asn37Leu, Asp39Thr, Gly123Leu, and Ala125Leu; Table S2) for the subsequent selection against the reduced dockerin library. Among a few hundred survived colonies, five were picked and the corresponding pTRG-Doc plasmids were isolated and reintroduced into the positive selection hosts that harbored either pBT-Coh_{wt} or pBT-Coh₁. Cell growth test confirmed that all five dockerin mutants engaged in strong interactions with Coh₁ and four out of five did not interact with Coh_{wt}. One dockerin mutant displayed moderate interaction with Coh_{wt}. Based on the colony size and growth rate on the positive selection plate, we chose a dockerin mutant (named as Doc₁; Ser11Arg, Thr12Pro, Ser45Pro, and Thr46Ala) for the following *in vitro* characterization.

In vitro characterization. Previous reports suggested that dockerin domain could not be produced as a discrete entity due to its degradation in *Escherichia coli*²². On the other hand, large quantity of dockerin domain could be obtained when it was co-expressed with cohesin^{22,41}. In addition, many reports showed that good expression of dockerin could be achieved when it was fused to well-folded proteins^{32–35}. To this end, dockerin domain variants (including its N-terminal X6b domain) were expressed as a C-terminal fusion to the maltose binding protein (MBP). A His₆ tag was added to the C-terminus of the fusion protein to facilitate the purification and ELISA experiments. Cohesin domain variants were purified as a C-terminal fusion to the glutathione S-transferase (GST). The GST tag improved expression of cohesin domains, facilitated protein purification, and did not interfere with the ELISA experiments using anti-His₆ antibody. We have also verified that GST does not interact with MBP.

To estimate the strength of interaction between cohesin and dockerin, we conducted semi-quantitative ELISA experiments. Briefly, wells of microtiter plates were coated with a GST-tagged cohesin. Different concentrations of the His₆-tagged dockerin of interest were then applied into each well. Following washing steps, the amounts of interacting dockerin were determined immunochemically using anti-His₆ antibody and HRP-labeled secondary antibody. As shown in Table 3, Doc₁ and Coh₁ displayed a strong mutual interaction with a K_d value of 4.57 ± 1.61 nM, which is comparable to that of the parent Doc_{wt}-Coh_{wt} pair (K_d = 0.77 ± 0.10 nM). On the other hand, the Doc₁-Coh₁ pair did not show obvious cross-interaction with the Doc_{wt}-Coh_{wt} pair. The K_d values of the Doc₁-Coh_{wt} and Doc_{wt}-Coh₁ cross pairs were too large to be accurately measured, which were estimated to be larger than 500 nM (Table 3 and Figure S4). The ELISA experiments confirmed that the Doc₁-Coh₁ pair is orthogonal to the parental Doc_{wt}-Coh_{wt} pair. To verify that the evolved Doc₁ mutant does not have increased level of non-specific interaction with other proteins due to a few hydrophilic-to-hydrophobic mutations, we conducted ELISA experiments between Doc₁ and a control protein, BSA. The K_d value of the Doc₁-BSA interaction was too large to be accurately measured. It is estimated to be larger than 1,500 nM, which is similar to that of the Doc_{wt}-BSA pair (K_d > 1000 nM; Figure S4). We therefore concluded that mutations in Doc₁ do not promote non-specific binding.

Conclusion. In summary, we have developed an approach to generate an interacting protein pair that is derived from but orthogonal to the parent protein pair. This is achieved by engineering the protein-protein interacting interface and facilitated by a combination of positive and negative selections in bacteria. To the best of our knowledge, our negative selection is the first example of applying URA3/5-FOA selection in a bacterial two-hybrid system. Presumably, more than one orthogonal protein pair can be generated with multiple cycles of positive and negative selections. The approach and tools that were developed in the current work can also potentially be applied to the generation of other orthogonally interacting proteins pairs of one's interest. These orthogonal protein pairs can potentially be applied to the assembly of artificial protein complexes both *in vitro* and *in vivo*. The precise control of relative contents and positions of building blocks within a protein assembly will likely facilitate the construction of protein complexes for protein-based nanomaterials or for efficient catalytic syntheses of bio-based chemicals through co-localization of enzymes

Methods

Materials and General Methods. Primers were ordered from Sigma. DNA sequencing services were provided by Eurofins MWG Operon. Restriction enzymes, antarctic phosphatase (AP) and T4 DNA ligase were purchased from New England Biolabs. KOD hot start DNA polymerase was purchased from EMD Millipore. Standard molecular biology techniques⁴² were used throughout. Site-directed mutagenesis was carried out using overlapping PCR. *E. coli* XL1-Blue MRF' was used in the construction and DNA propagation of all plasmids that were derived from pBT and pTRG vectors. *E. coli* GeneHogs were used for routine cloning and DNA propagation

of all other plasmids. All solutions were prepared in deionized water that was further treated by Barnstead Nanopure® ultrapure water purification system (Thermo Fisher Scientific Inc). LB medium (1 L) contained Bacto tryptone (10 g), Bacto yeast extract (5 g), and NaCl (10 g). M9 salts (1 L) contained Na₂HPO₄ (6 g), KH₂PO₄ (3 g), NH₄Cl (1 g), and NaCl (0.5 g). M9 glucose medium contained glucose (10 g), MgSO₄ (0.12 g), CaCl₂ (0.028 g) and thiamine hydrochloride (0.001 g) in 1 L of M9 salts. Antibiotics were added where appropriate to following final concentrations: ampicillin, 100 mg L⁻¹; kanamycin, 50 mg L⁻¹; chloramphenicol, 25 mg L⁻¹; tetracycline, 12.5 mg L⁻¹. The 6xHis tag monoclonal antibody was purchased from Thermo Fisher Scientific. The goat anti-mouse IgG-HRP conjugate was purchased from BioRad.

Plasmid construction. Plasmid pBT-Coh_{wt} was constructed by inserting Coh_{wt}-encoding gene (the second cohesin domain from CipA; residues 182–328) between the *EcoRI* and *BamHI* sites of the pBT vector. Coh_{wt}-encoding gene was PCR amplified using primers P1 and P2 (Table S1) from the chromosomal DNA of ATCC 27405.

Plasmid pTRG-Doc_{wt} was constructed by inserting Doc_{wt}-encoding gene (the dockerin domain from xylanase 10B; residues 733–791) between the *BamHI* and *XhoI* sites of the pTRG vector. Doc_{wt}-encoding gene was PCR amplified using primers P3 and P4 (Table S1) from the chromosomal DNA of ATCC 27405. DNA sequence that encodes X6b carbohydrate binding domain was included at the 5' end of the Doc_{wt}-encoding gene.

Plasmid pTRG-Doc_{AL} was constructed by site-directed mutagenesis of plasmid pTRG-Doc_{wt}. Mutations (Ser11Ala, Thr12Leu, Ser45Ala, and Thr46Leu) were introduced by overlapping PCR using primers P5, P6, P7, P8, and P9 (Table S1). The resulting DNA fragment was inserted into the pTRG vector using Ligation Independent Cloning (SLIC)⁴³.

Plasmids pGEX-Coh_{wt} and pGEX-Coh₁ were constructed by inserting Coh_{wt}-encoding gene and Coh₁-encoding gene between the *EcoRI* and *XhoI* sites of pGEX vector, respectively. As a result, the cohesin variants were expressed as fusion protein to the C-terminus of GST. The Coh_{wt}-encoding gene and Coh₁-encoding gene were amplified using primers P10 and P11 (Table S1).

Plasmids pMAL-Doc_{wt}, pMAL-Doc_{AL}, and pMAL-Doc₁ were constructed by inserting a dockerin gene of interest between the *BamHI* and *XhoI* sites of pMAL vector, respectively. The dockerin variants were expressed as C-terminus fusion of MBP. The dockerin encoding genes were amplified using primers P3 and P12 (Table S1).

Construction of a dockerin library. Four residues (Ser11, Thr12, Ser45, and Thr46) of dockerin were randomized. Primers P29 and P30 (Table S1) were used to introduce these mutations. The full-length dockerin mutant fragments were assembled by overlapping PCR of the above two DNA fragments using primers P3 and P4 (Table S1). The resulting DNA was digested with *BamHI* and *XhoI*, and subsequently cloned into the pTRG vector that was digested with the same pair of restriction enzymes to produce the dockerin library.

Construction of a cohesin library. Four residues (Asn37, Asp39, Gly123, and Ala125) of cohesin that are in contact with the Ser/Thr motif of dockerin were randomized. Primers P13 and P14 (Table S1) were used to amplify a DNA fragment that contains mutations at positions Gly123 and Ala125. Primers P15 and P16 were used to amplify a DNA fragment that contains mutation at positions Asn37 and Asp39. The full-length cohesin mutant fragments were assembled by overlapping PCR of the above two DNA fragments using primers P1 and P2 (Table S1). The resulting DNA was digested with *EcoRI* and *BamHI*, and subsequently cloned into the pBT vector that was digested with the same pair of restriction enzymes to produce the cohesin library.

Construction of host strain for negative selection. Chromosomal deletion and modification of the F' plasmid was carried out using the phage λ Red-mediated homologous recombination⁴⁴. In brief, an appropriate *E. coli* host strain was first transformed with plasmid pRed-ET (Gene Bridges). A single colony of transformed cells was cultured in LB medium containing Ap at 30 °C. Expression of the λ Red recombination proteins was induced with L-arabinose at a final concentration of 0.4% (wt/vol), when the cell growth reached the mid exponential phase. The cultivation temperature was shifted to 37 °C. Following additional 1 h of growth, the cells were harvested for the preparation of recombination-ready electrocompetent cells. To knockout the chromosomal *pyrF* gene (encodes orotidine-5'-phosphate decarboxylase), linear DNA fragment was assembled by overlapping PCR using primers P17, P18, P19, P20, P21, and P22. The DNA contains a chloramphenicol acetyltransferase-encoding gene flanked by DNA sequences (50–60 bp) that are homologous to the upstream and downstream regions of the *pyrF* gene. Following transformation into the BacterioMatch II reporter strain, successful gene deletion event was selected by plating cells on solid media containing chloramphenicol. The chloramphenicol acetyltransferase selection marker was subsequently removed from the genome using FLP recombinase⁴⁴ to yield strain WNPP17, which is a uridine auxotroph. Insertion of the URA3 gene behind the HIS3 reporter gene on the F' plasmid of WNPP17 was achieved by electroporation of DNA fragment that was constructed by overlapping PCR using primers P23, P24, P25, P26, P27, and P28. Successful gene insertion event led to the recovery of the uridine auxotrophic phenotype. Strains grown on M9 media containing glucose as the sole carbon source were evaluated and characterized to result in WNPP18.

Negative selection. The negative selections were performed to eliminate the cohesin and the dockerin mutants that could interact with Doc_{wt} and Coh_{wt}, respectively. For negative selection with the cohesin library, WNPP18 cells containing pBT-Coh_{lib} and pTRG-Doc_{wt} were cultivated in 5 mL LB medium overnight. The overnight culture (1 mL) was collected using a tabletop centrifuge at 2000 g for 10 minute at room temperature. After removal of the LB medium, cells were washed once using 1 mL of M9 complete medium (1 × M9 salts, 1 mM MgSO₄, 0.1 mM CaCl₂, 10 mg/L thiamine, 0.01 mM ZnSO₄, 0.2 mM uracil, 1 g/L histidine, 0.01% yeast extract, 0.4% D-glucose), then re-suspended in 1 mL of the same medium. The cells were incubated at 37 °C for 2 hours

with shaking (225 rpm), which allowed cells to adapt to the growth in minimal medium before plating. Around 5×10^6 cells were plated on M9 complete medium plates containing 2.5 mM 5-FOA, 0.05 mM IPTG, and appropriate concentrations of chloramphenicol and tetracycline. After 36 h of incubation at 37 °C, cells were collected from the plate into 1 mL M9 complete medium. Plasmid DNA was extracted from the collected cells. Mixture of the pBT-Coh_{lib} and pTRG-Doc_{wt} plasmids was first treated by restriction enzyme to linearize the pTRG-Doc_{wt} plasmid. The pBT-Coh_{lib} plasmids were then isolated by DNA gel electrophoresis purification. Negative selection with the dockerin library was conducted using the same procedure.

Positive selection. For positive selections with the reduced cohesin library, the pBT-Coh_{lib} from the negative selection was transformed into the BacterioMatch II reporter strain containing a pTRG-Doc variant of interest. The positive selection followed instructions of the BacterioMatch II two-hybrid kit. In brief, overnight bacterial culture in LB medium (1 mL) was collected by centrifugation. Cell pellets were washed with M9-His drop medium (1×10^9 salts, 1 mM MgSO₄, 0.1 mM CaCl₂, 10 mg/L thiamine, 0.001 mM ZnSO₄, 1×10^9 His-drop supplement, 0.2 mM adenine, 0.4% D-glucose) to completely remove the residue LB medium. Cells were then re-suspended in 1 mL M9-His drop medium and incubated for 2 h at 37 °C with shaking (225 rpm). An aliquot of cells (3×10^6) was plated on M9-His drop medium plates containing 5 mM 3-AT, 0.05 mM IPTG, and appropriate concentrations of chloramphenicol and tetracycline. Positive selections with the reduced dockerin library followed the same procedure.

Enzyme-linked immunosorbent assay (ELISA). MaxiSorp 96 well ELISA plates were coated overnight at 4 °C with 100 µL of the desired protein (30 nM in 0.1 M Na₂CO₃ (pH 9.6)). Following steps were all performed at a volume of 100 µL/well at room temperature unless otherwise stated. After removal of the coating solution, blocking buffer (1 mM CaCl₂ and 1% BSA in TBS buffer) was added and the plates were incubated for 1 h. The plates were washed three times with washing buffer (blocking buffer supplemented with 0.05% Tween 20 without BSA; 200 µL/well per wash). Potential binding partner of the coating protein (10 pM–1 µM in blocking buffer) was applied to each well. The plates were again incubated for 1 h followed by washing for three times. Primary antibody (anti-6xHis, 1:500 dilution in blocking buffer) was added and incubated for 1 h. Plates were washed. Secondary antibody (goat anti-mouse IgG-HRP conjugate, 1:500 dilution in blocking buffer) was added for the final incubation of 1 h followed by washing for three times. Quantification of the HRP activity used the 3, 3', 5, 5'-tetramethylbenzidine (TMB) substrate. The reaction was initiated by the addition of 100 µL/well TMB. After 5 min of reaction or until the desired color development achieved, 50 µL/well of 1 M H₂SO₄ was added to terminate the reaction. Absorbance at 450 nm was measured. Dissociation constants were calculated by curve fitting with Hill Equation using MATLAB (R2016b).

References

- Lovejoy, B. *et al.* Crystal structure of a synthetic triple-stranded alpha-helical bundle. *Science* **259**, 1288–1293 (1993).
- Harbury, P. B., Plecs, J. J., Tidor, B., Alber, T. & Kim, P. S. High-resolution protein design with backbone freedom. *Science* **282**, 1462–1467 (1998).
- Gribbon, C. *et al.* MagicWand: A single, designed peptide that assembles to stable, ordered α -helical fibers. *Biochemistry* **47**, 10365–10371 (2008).
- Zaccai, N. R. *et al.* A de novo peptide hexamer with a mutable channel. *Nat. Chem. Biol.* **7**, 935–941 (2011).
- Koder, R. L. *et al.* Design and engineering of an O₂ transport protein. *Nature* **458**, 305–309 (2009).
- Ballister, E. R., Lai, A. H., Zuckermann, R. N., Cheng, Y. & Mougous, J. D. *In vitro* self-assembly of tailorable nanotubes from a simple protein building block. *Proc. Natl. Acad. Sci. USA* **105**, 3733–3738 (2008).
- Usui, K. *et al.* Nanoscale elongating control of the self-assembled protein filament with the cysteine-introduced building blocks. *Protein Sci.* **18**, 960–969 (2009).
- Ringler, P. & Schulz, G. E. Self-assembly of proteins into designed networks. *Science* **302**, 106–109 (2003).
- Salgado, E. N., Faraone-Mennella, J. & Tezcan, F. A. Controlling protein-protein interactions through metal coordination: Assembly of a 16-helix bundle protein. *J. Am. Chem. Soc.* **129**, 13374–13375 (2007).
- Salgado, E. N., Radford, R. J. & Tezcan, F. A. Metal-directed protein self-assembly. *Acc. Chem. Res.* **43**, 661–672 (2010).
- Brodin, J. D. *et al.* Metal-directed, chemically tunable assembly of one-, two- and three-dimensional crystalline protein arrays. *Nat. Chem.* **4**, 375–382 (2012).
- Grigoryan, G. *et al.* Computational design of virus-like protein assemblies on carbon nanotube surfaces. *Science* **332**, 1071–1076 (2011).
- Padilla, J. E., Colovos, C. & Yeates, T. O. Nanohedra: Using symmetry to design self assembling protein cages, layers, crystals, and filaments. *Proc. Natl. Acad. Sci. USA* **98**, 2217–2221 (2001).
- Sinclair, J. C., Davies, K. M., Venien-Bryan, C. & Noble, M. E. M. Generation of protein lattices by fusing proteins with matching rotational symmetry. *Nat. Nanotechnol.* **6**, 558–562 (2011).
- Douglas, T. & Young, M. Viruses: Making friends with old foes. *Science* **312**, 873–875 (2006).
- Tanaka, S. *et al.* Atomic-level models of the bacterial carboxysome shell. *Science* **319**, 1083–1086 (2008).
- Bayer, E. A., Belaich, J.-P., Shoham, Y. & Lamed, R. The cellulosomes: Multienzyme machines for degradation of plant cell wall polysaccharides. *Annu. Rev. Microbiol.* **58**, 521–554 (2004).
- Gilbert, H. J. Cellulosomes: microbial nanomachines that display plasticity in quaternary structure. *Mol. Microbiol.* **63**, 1568–1576 (2007).
- Doi, R. H. & Kosugi, A. Cellulosomes: plant-cell-wall-degrading enzyme complexes. *Nat. Rev. Microbiol.* **2**, 541–551 (2004).
- Janin, J., Bahadur, R. P. & Chakrabarti, P. Protein-protein interaction and quaternary structure. *Q. Rev. Biophys.* **41**, 133–180 (2008).
- Nikitin, M. P., Zdobnova, T. A., Lukash, S. V., Stremovsky, O. A. & Deyev, S. M. Protein-assisted self-assembly of multifunctional nanoparticles. *Proc. Natl. Acad. Sci. USA* **107**, 5827–5832 (2010).
- Carvalho, A. L. *et al.* Cellulosome assembly revealed by the crystal structure of the cohesin-dockerin complex. *Proc. Natl. Acad. Sci. USA* **100**, 13809–13814 (2003).
- Smith, G. P. Filamentous fusion phage: novel expression vectors that display cloned antigens on the virion surface. *Science* **228**, 1315–1317 (1985).
- Boder, E. T. & Wittrup, K. D. Yeast surface display for screening combinatorial polypeptide libraries. *Nat. Biotechnol.* **15**, 553–557 (1997).
- Daugherty, P. S. Protein engineering with bacterial display. *Curr. Opin. Struct. Biol.* **17**, 474–480 (2007).
- Fields, S. & Song, O. A novel genetic system to detect protein-protein interactions. *Nature* **340**, 245–246 (1989).

27. Dove, S. L. & Hochschild, A. Conversion of the ω subunit of *Escherichia coli* RNA polymerase into a transcriptional activator or an activation target. *Genes Dev.* **12**, 745–754 (1998).
28. Dove, S. L., Joung, J. K. & Hochschild, A. Activation of prokaryotic transcription through arbitrary protein-protein contacts. *Nature* **386**, 627–630 (1997).
29. Joung, J. K., Ramm, E. I. & Pabo, C. O. A bacterial two-hybrid selection system for studying protein-DNA and protein-protein interactions. *Proc. Natl. Acad. Sci. USA* **97**, 7382–7387 (2000).
30. Vidal, M., Brachmann, R. K., Fattaey, A., Harlow, E. & Boeke, J. D. Reverse two-hybrid and one-hybrid systems to detect dissociation of protein-protein and DNA-protein interactions. *Proc. Natl. Acad. Sci. USA* **93**, 10315–10320 (1996).
31. Boeke, J. D., LaCroute, F. & Fink, G. R. A positive selection for mutants lacking orotidine-5'-phosphate decarboxylase activity in yeast: 5-fluoro-orotic acid resistance. *Mol. Genet.* **197**, 345–346 (1984).
32. Haimovitz, R. *et al.* Cohesin-dockerin microarray: diverse specificities between two complementary families of interacting protein modules. *Proteomics* **8**, 968–979 (2008).
33. Karpol, A., Barak, Y., Lamed, R., Shoham, Y. & Bayer, E. A. Functional asymmetry in cohesin binding belies inherent symmetry of the dockerin module: insight into cellulosome assembly revealed by systematic mutagenesis. *Biochem. J.* **410**, 331–338 (2008).
34. Barak, Y. *et al.* Matching fusion protein systems for affinity analysis of two interacting families of proteins: The cohesin-dockerin interaction. *J. Mol. Recognit.* **18**, 491–501 (2005).
35. Fierobe, H.-P. *et al.* Design and production of active cellulosome chimeras. Selective incorporation of dockerin-containing enzymes into defined functional complexes. *J. Biol. Chem.* **276**, 21257–21261 (2001).
36. Meng, X. & Wolfe, S. A. Identifying DNA sequences recognized by a transcription factor using a bacterial one-hybrid system. *Nat. Protoc.* **1**, 30–45 (2006).
37. Schaeffer, F. *et al.* Duplicated dockerin subdomains of *Clostridium thermocellum* endoglucanase CelD bind to a cohesin domain of the scaffolding protein CipA with distinct thermodynamic parameters and a negative cooperativity. *Biochemistry* **41**, 2106–2114 (2002).
38. Mechaly, A. *et al.* Cohesin-dockerin recognition in cellulosome assembly: experiment versus hypothesis. *Proteins: Struct., Funct., Genet.* **39**, 170–177 (2000).
39. Mechaly, A. *et al.* Cohesin-dockerin interaction in cellulosome assembly: a single hydroxyl group of a dockerin domain distinguishes between nonrecognition and high affinity recognition. *J. Biol. Chem.* **276**, 9883–9888 (2001).
40. Schaeffer, F. *et al.* Duplicated dockerin subdomains of *Clostridium thermocellum* endoglucanase CelD bind to a cohesin domain of the scaffolding protein CipA with distinct thermodynamic parameters and a negative cooperativity. *Biochemistry* **41**, 2106–2114 (2002).
41. Carvalho, A. L., Dias, F. M. V., Nagy, T., Prates, J. A. M. & Proctor, M. R. Evidence for a dual binding mode of dockerin modules to cohesins. *Proc. Natl. Acad. Sci. USA* **104**, 3089–3094 (2007).
42. Sambrook, J. F., Russell, D. W. & Editors. *Molecular cloning: A laboratory manual, third edition*. (Cold Spring Harbor Laboratory Press, 2000).
43. Li, M. Z. & Elledge, S. J. Harnessing homologous recombination *in vitro* to generate recombinant DNA via SLIC. *Nat. Methods* **4**, 251–256 (2007).
44. Datsenko, K. A. & Wanner, B. L. One-step inactivation of chromosomal genes in *Escherichia coli* K-12 using PCR products. *Proc. Natl. Acad. Sci. USA* **97**, 6640–6645 (2000).

Acknowledgements

This work is supported by the New Faculty Startup Fund to J. Guo from the Chemistry Department of University of Nebraska – Lincoln, by cycle-5 grant from the Nebraska Center For Energy Sciences Research (to J.G. and W.N.), and by Grant CBET 1264708 (to J.G. and W.N.) from NSF.

Author Contributions

J.L. constructed plasmids, performed protein purification and *in vitro* characterization. X.S. constructed plasmids, performed selection and protein purification. W.N. constructed libraries, devised the negative selection, and wrote the manuscript. J.G. designed the study and wrote the manuscript.

Additional Information

Supplementary information accompanies this paper at <https://doi.org/10.1038/s41598-018-19281-6>.

Competing Interests: The authors declare that they have no competing interests.

Publisher's note: Springer Nature remains neutral with regard to jurisdictional claims in published maps and institutional affiliations.



Open Access This article is licensed under a Creative Commons Attribution 4.0 International License, which permits use, sharing, adaptation, distribution and reproduction in any medium or format, as long as you give appropriate credit to the original author(s) and the source, provide a link to the Creative Commons license, and indicate if changes were made. The images or other third party material in this article are included in the article's Creative Commons license, unless indicated otherwise in a credit line to the material. If material is not included in the article's Creative Commons license and your intended use is not permitted by statutory regulation or exceeds the permitted use, you will need to obtain permission directly from the copyright holder. To view a copy of this license, visit <http://creativecommons.org/licenses/by/4.0/>.

© The Author(s) 2018